Improving the performance of heterojunction silicon solar cells from the band diagram and surface passivation

BODOLALAINA Randriamanalina[1], RASTEFANO Elisée[2]

[1]*PhD student, SE-I-MSDE, ED-STII, Antananarivo, Madagascar*
[2]*Thesis Director, SE-I-MSDE, ED-STII, Antananarivo, Madagascar*

ABSTRACT

Research activities have made it possible to achieve high efficiency for heterojunction cells. Among the improvements that contribute to the higher efficiency. Passivation of the c-Si substrate surface by a thin intrinsic layer of a-Si:H is deposited between the a-Si:H layer and the c-Si substrate. This configuration is known as intrinsic thin film heterojunction (HIT) solar cells. Various research methodologies used to improve the efficiency of HIT cells have been developed over the years and HIT cells with efficiencies greater than 24% are currently being fabricated. A number of characterisations have been established to ensure development which are based on the evaluation of effective carrier lifetime, interface state density, recombination rate, cell efficiency, band gap, current density-voltage characteristics, charge carrier concentration, photoluminescence, activation energy, etc. But the quality of surface passivation plays a crucial role in the performance of heterojunction solar cells. This paper reports on the estimated improvements responsible for the development of these solar cells.

Keywords*: a-Si:H, c-Si, heterojunction solar cell, band diagram, surface passivation*

1 Introduction

Hydrogenated amorphous silicon/crystalline silicon (aSi:H/c-Si) heterojunction solar cells with an intrinsic buffer layer were studied, to explain the effect of energy band shift, as well as the passivation quality on the performance of aSi:H/c-Si heterojunction solar cells. The objective is to understand the factor that impacts on the conversion efficiency of these cells. In figure 1, An "S-shaped" deformation of the J-V characteristics is observed in defiance of the surface passivation quality for single-layer intrinsic high-energy bandgap (Eg > 3.0 eV) heterojunction solar cells.

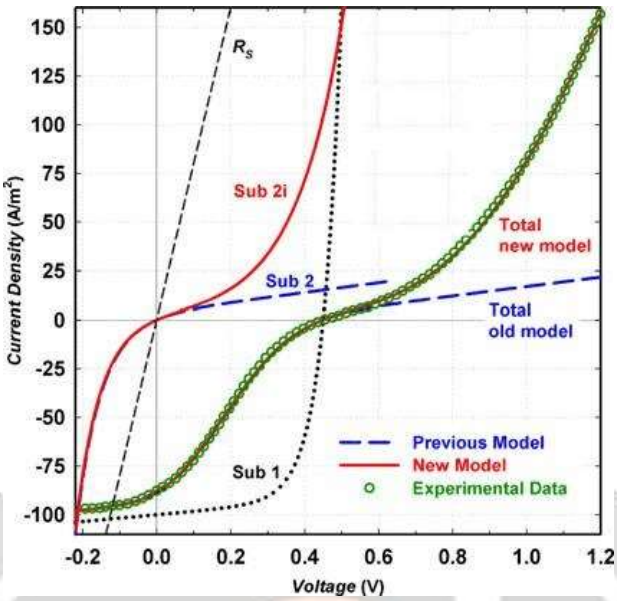

Figure 1: S-shaped I-V caracteristic heterojunction solar cell

Typical configurations of heterojunction and HIT solar cells are shown in figure 2, and configured as follows:TCO(SnO2)/aSi:H(p)/c-Si(n)/a-Si:H(n+)/TCO(ZnO)/Ag,TCO/ aSi:H(p)/a-Si:H(i)/c-Si(n)/a-Si:H(i)/a-Si:H(n+)/TCO/Al and bifacial HIT solar cell, i.e. TCO/a-Si:H(p)/a-Si:H(i)/c-Si(n)/aSi:H(i)/a-Si:H(n+)/TCO/Al.

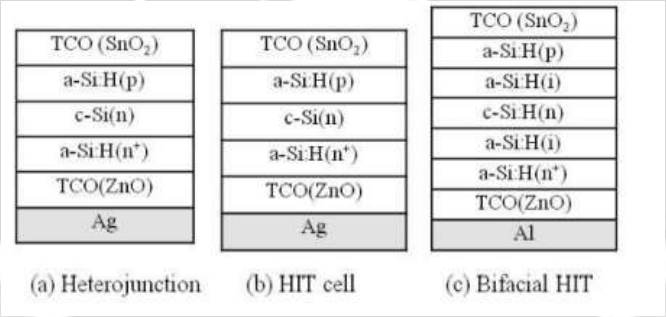

Figure 2: Different forms of heterojunction cell

The collection probability of the photogenerated holes as well as the accumulation of holes (electrons) and the trapping of holes (electrons) at the a-Si:H/c-Si interface strongly depend on the magnitude of the band bending shift discontinuity at the a-Si:H/c-Si interface.

2 Band diagram of a-Si:H /c-Si

The a-Si:H/c-Si heterojunction is mainly used to make photovoltaic cells. It is a heterojunction between an amorphous material (i.e. with a direct gap) and a crystalline material with an indirect gap. For heterojunctions, the basic model is the Anderson model which is without interface states. This basic model is incomplete because charge transport in heterojunction devices can be dominated by trapping phenomena at interface states.

The electron affinity qχ is the energy required to extract an electron from the conduction band to the vacuum level. It is 4.05 eV for crystalline silicon and 3.87 eV for amorphous silicon. The Fermi level varies with temperature and especially with doping. The band gap of crystalline silicon is 1.12 eV at 300 K and that of hydrogenated amorphous silicon is between 1.55 eV and 2.10 eV [01].

The following diagram shows a band diagram of a (p)aSi:H/(n)c-Si heterojunction. Because of the difference in bandgap of the two semiconductors, we have :

$$\Delta E_V = E_V^{c-Si} - E_V^{a-Si:H} \quad (1)$$

and a conduction band edge gap quantified by :

$$\Delta E_C = E_C^{a-Si:H} - E_C^{c-Si} \quad (2)$$

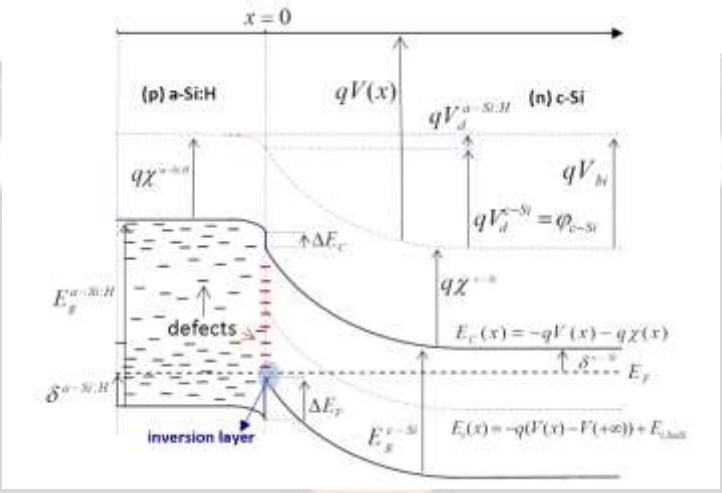

Figure 3: Schematic diagram of the equilibrium position of the E_C conduction and E_V valence bands with respect to the position of the Fermi E_F level for a (p)a-Si:H/(n)c-Si heterojunction.

Band gaps are inseparable from heterojunctions and are the consequence of the difference in gaps. The doping of the semiconductors modifies the diffusion potentials but hardly any of the band discontinuities. In Figure 3, the discontinuities are divided between the conduction band discontinuity ΔEc and the valence band discontinuity ΔEv. The algebraic sum of these two discontinuities is equal to the difference of the gaps ΔE, i.ge.

$$\Delta E_g = \Delta E_c + \Delta E_v \quad (3)$$

The addition of a larger gap hydrogenated amorphous silicon layer following a smaller gap layer (e.g. crystalline silicon) leads to the formation of a heterojunction. The large optical gap of amorphous silicon compared to crystalline silicon allows for reduced absorption losses and since the doped layers have properties such that the photogenerated carriers recombine rapidly. The band discontinuity prevents electrons from backscattering and thus reduces recombination losses. The final structure depends on several parameters of the two materials in contact which are: the value of the $E_{g1}$and E_{g2} bandgaps, the electron affinities and the$\chi_1\chi_2$ doping levels. The transport properties of carriers in heterojunctions are generally dominated by trapping phenomena at the interface between the n- and p-regions [02].

Anderson's model generalized the drift-diffusion model to heterojunctions [03]

3 Intrinsic layer a-Si: H(i) for passivation

In figure 4, inserting an undoped (intrinsic) a-Si:H layer between the c-Si substrate and the doped a-Si:H layer increases the surface passivation and thus the V_{co} of the cell. The small thickness of this intrinsic a-Si:H layer does not disturb the electric field while decreasing the defect density at the interface [04].

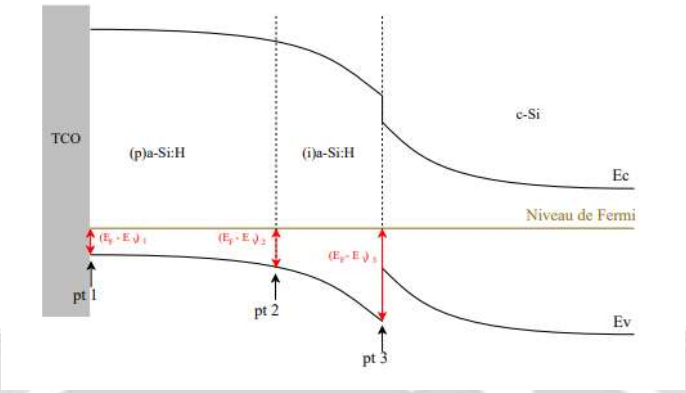

Figure 4: Schematic of a bending of the E_V valence and E_C conduction bands on a PIn structure. The gap between the Fermi level E_F and E_V is shown at the TCO/(p) a-Si:H interface (pt 1), at the (p) a-Si:H/(i) a-Si:H interface (pt 2) and at the (i)a-Si:H/c-Si interface (pt 3)

4 Theoretical predictions of band discontinuity or band offset

The ability to find a reference energy level is ideal for each material. Two theories are used to predict band shifts :

- **Anderson's rule: the vacuum level**

Anderson's rule states that the void level of the two materials must be aligned at the interface. The key parameter is the electronic affinity, defined as the energy distance between the bottom of the conduction band and the vacuum level. The band shifts are then determined by the differences in electron affinity and band gap, as schematically shown in Figure 05, as given by equations (4) and (5):

$$\Delta E_C = \chi_{c-Si} - \chi_{a-Si:H} \quad (4)$$

$$\Delta E_v = E_g^{a-Si} - E_g^{c-Si} - \Delta E_C \quad (5)$$

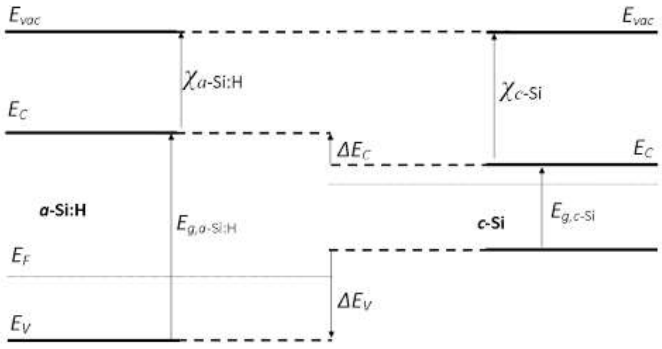

Figure 5: Alignment of vacuum levels at the a-Si:H/ c-Si interface, in the framework of Anderson's theory. Fermi level balancing occurs by charge transfer when the materials are in contact [05]

One of the main weaknesses of Anderson's rule is that electronic affinity is a surface property: its use at the interface between two semiconductors is not desirable. Moreover, microscopic dipoles could arise from localized charge transfer at the interface and play a role in band alignment. And again, Anderson's model fails to describe metal/semiconductor contacts, a special case of heterojunctions [06]. As a result, Anderson's rule is an oversimplified theory used to quickly obtain an imperfect estimate of the band offset.

- **The branch point theory**

At the surface of a material, the periodicity of the crystal structure is broken. Interface-induced vacuum states, arising from complex solutions of the Schrödinger equation at the surface, escape into the vacuum or into the neighboring material [07]. These defects, originating from the bulk band diagram, are mainly of donor type near the valence band edge and acceptor type near the conduction band edge. The branching point (BP), or charge neutrality level (CNL), is defined as the energy point where the states switch from donor to acceptor dominance. This is a neutrality point: if the Fermi level coincides with this point, the interface-induced defects does not present net charge [19].

Calculations by Tersoff using the augmented plane wave method place the CNL of crystalline silicon at 0.36 eV from the valence band edge [08], while Flores places it at 0.63 eV on the basis of experimental measurements of barrier heights.

The branch point theory, first introduced by Tejedor and Flores [09], takes the branch point φ_{bp}^{X} in semiconductor as the reference level in figure. 6. The band shifts are then calculated, from equations (6) and (7):

$$\Delta E_C = E_g^{a-Si} - E_g^{a-Si} + \Delta_{dip} \quad (6)$$

$$\Delta E_v = E_g^{a-Si} - E_g^{c-Si} - \Delta E_v \quad (7)$$

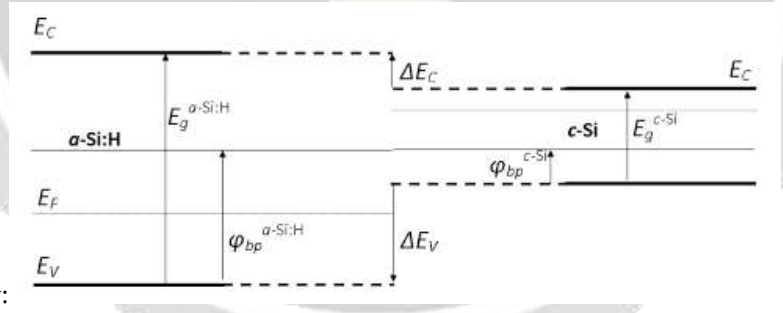

by:

Figure 6: Alignment of branch points at the a-Si:H/ c-Si interface, within the framework of the Bardeen rule. The fermi level equilibrium occurs by charge transfer when the materials are in contact [05].

Δ_{dip} accounts for the presence of interface dipoles, forcing the potential down over a few Angstroms; this can be represented by an additional contribution to band shifts.

- **Effect of hydrogen in band discontinuities**

The band discontinuities of the a-Si:H/c-Si system is very noticeable for heterojunction cells... There are probably a multiplicity of parameters that can modify these discontinuities. Hydrogen is among the major contributors to this band discontinuity effect and passivation.

The first demonstration of a massive modification of band discontinuities by atomic hydrogen is due to Perfetti et al [10] in a system "close" to ours since it is the SiO2/Si heterojunction. A significant ΔE_v drop of 0.5 eV was obtained using a fine layer at the SiO2/Si interface. These are experiments and the influence of dipoles at this SiO2/Si interface is discussed using a simple model [11].

ChrisG. VandeWalle et al. studied the theoretical dependence of the band discontinuities of the system corresponding to a-Si:H/c-Si cells [12]. Their ab initio calculations showed a considerable quantitative effet of the hydrogen content of a-Si:H in contact with c-Si on the band discontinuities. It is stated that it is the hydrogen content of the few atomic layers of the a-Si:H near the interface that is relevant and to be considered in the discontinuity calculations.

These calculations show that the discontinuities are very sensitive to the hydrogen content and that the valence band of a-Si:H is lowered by an average of 40 meV per additional percent of hydrogen in the a-Si:H near the interface.

6 Basic modelling equations

The basic equations are:

- the Poisson equation,
- the two current equations and
- the two continuity equations.

Poisson's equation relates variations in electrostatic potential to local charge densities. The continuity and transport equations describe how electron and hole densities change as a function of transport, generation and recombination mechanisms. By solving these basic equations, the distributions of electrons, holes, potential and space charge can be found simultaneously. A system of five basic equations can be reduced to a system of three equations because the two current equations are ndeed included in the two continuity equations. The numerical simulation is based on the solution of these three fundamental equations that govern the charge transport in semiconductors: Poisson equation and continuity equations for electrons and holes.

- **Poisson's equation**

The Poisson equation is defined below :

where φ is the electrostatic potential, , $\nabla(.)$ is the gradient vector, ε is the local permittivity of the medium, $\vec{r}$ is the position vector and ρv is the volume charge density. The electric field is deduced from the gradient of the electrostatic potential by:

$$\vec{E} = -\nabla\varphi \qquad (8)$$

- **Continuity equations**

The charge carrier continuity equations describe the evolution of the concentration of electrons and holes as a function of time. The variation of the local concentration of a carrier (electron or hole) can have different origins [08]: The band gap of a semiconductor may be small enough to allow the direct transition of electrons and holes between the conduction band and the valence band, or between these bands and the energy levels created by defects or impurities located within the band gap. These generation and recombination phenomena can be of internal (thermal agitation) or external (external source) origin. An external source of carrier generation can cause an increase in the local concentration of electrons or holes. A typical example of carrier generation by an external source is the creation of electron-hole pairs under the influence of light. Transport phenomena with the presence of conduction or diffusion currents. The continuity equations for electrons and holes are given by the following expressions [13]

$$\frac{\partial n}{\partial t} = \frac{1}{q}\frac{\partial \vec{j_n}}{\partial t}(\vec{r}, t) + G_n(\vec{r}) - R_n(\vec{r}) \quad (9)$$

$$\frac{\partial p}{\partial t} = \frac{1}{q}\frac{\partial \vec{j_p}}{\partial t}(\vec{r}, t) + G_p(\vec{r}) - R_p(\vec{r}) \quad (10)$$

Where: q is the absolute value of the elementary electronic charge, n and p are the concentrations of electrons and holes. $\vec{j}_n(\vec{r},t)$ and $\vec{j}_p(\vec{r},t)$ are the electron and hole current densities, $G_n(\vec{r})$ and $G_p(\vec{r})$ are the electron and hole generation rates, $R_n(\vec{r})$ and $R_p(\vec{r})$ are the recombination rates of electrons and holes.

In semiconductor physics, carrier generation and recombination are mechanisms through which mobile electrons and holes are created and eliminated. These mechanisms are fundamental to the operation of semiconductor devices.

In steady stable situation, the equations simplify to:

$\frac{\partial n}{\partial t} = 0$ and $\frac{\partial p}{\partial t} = 0$ which means that the carrier concentrations are only a function of the position

- **Transport equations**

The basic equations provide a general framework but the secondary equations will allow the determination of specific physical models for the following variables $\vec{j}_n, \vec{j}_p$, G_n, G_p, R_n, R_p.The existence of electric currents in a semiconductor is explained by the presence of an electric field and also by a concentration gradient of charge carriers in the semiconductor.

This phenomenon leads to the drift equation model commonly used to describe charge transport model is semiconductor.

Thus, the current densities $\vec{j}_n$ and $\vec{j}_p$ of the continuity equations can be approximated using Boltzmann transport theory by the diffusion drift model

Using the quasi-Fermi levels of electrons and holes (E_{Fn} and E_{Fp}) their expressions are :

$$\vec{j}_n = \mathbf{q\mu_n n \vec{\nabla} E_{Fn}} \quad (11)$$

$$\vec{j}_p = \mathbf{q\mu_p p \vec{\nabla} E_{Fp}} \quad (12)$$

Where μ_n and μ_p are the electron and hole mobilities, (E_{Fn} and E_{Fp}) are the quasi-Fermi levels of the electrons and holes

7 Conclusion

The results obtained revealed the appearance of an S-shaped J-V curve, when a high energy bandgap material (Eg > 3.0 eV) is used as an intrinsic buffer layer. This could be attributed to the accumulation of holes at the interface, which leads to surface recombination and, consequently, a reduction in cell performance. The S-shaped J-V disappeared at a reduced energy band gap value ≤1.72 eV. In this bandgap region, the device performance depends on the quality of the surface passivation. The high minority carrier lifetime measured at the interface leads to a high Voc, as well as FF, and thus a better efficiency of the solar cell.

REFERENCES

[1] M. Rahmouni, A. Datta, P. Chatterjee, J. Damoon-Lacoste, C. Ballif, P. Roca i Cabarrocas, J. Appl. Phys. 107, 054521 (2010).
[2] Wenham S. R., Green M. A. and Watt M. E, «Applied Photovoltaic», Bridge Printer, Sidney, (1994).2015
[3] S. M. Sze & K. Ng Kwok. Physics of semiconductor devices. John Wiley & Sons, 3 edition, 2007.
[4] H. Mathieu. « Physique des semi-conducteurs et des composants électroniques», Dunod, Paris, 2009.2017
[5] R. Varache, Doktor der Naturwissenschaften, "Development, characterization and modeling of interfaces for high efficiency silicon heterojunction solar cells", Berlin 2013
[6] S. M. Sze & K. Ng Kwok. Physics of semiconductor devices. John Wiley & Sons, 3 edition, 2007
[7] W. Moench. Semiconductor surfaces and interfaces. Springer, 2001).
[8] J. Tersoff. Theory of semiconductor heterojunctions: The role of quantum dipoles. Phys. Rev. B, vol. 30
[9] C. Tejedor & F. Flores. A simple approach to heterojunctions. J. Phys. C Solid State, vol. 11, pages L19–23, 1978.
[10] Trends in photovoltaic applications,(1992-2005). Technical report, IEA Photovoltaic Power Systems Program, (September 2006).
[11] Djicknoum DIOUF, « Cellules photovoltaïques silicium à hétérojonctions et à structure interdigitée en face arrière », Thèse doctorat, Université paris 2010.
[12] Frédéric Fossard « Spectroscopie infrarouge des fils et boîtes quantiques d'lnAS/InALS/Inp (001) these présentée pour obtenir le grade de docteur en science.
[13] ECHERI Abdelssalem, « Mémoire fin d'étude simulation d'une cellule photovoltaïque à base d'hétérojonction », Université KASDI MERBAH, Ouargla, 2015